Study of the ultrametric structure of Finite Dimensional Spin Glasses throught a constrained Monte Carlo dynamic

A. Cacciuto

Dipartimento di Fisica and Infn, Università di Cagliari

Via Ospedale 72, 09100 Cagliari (Italy)

E-mail cacciuto@vaxca.ca.infn.it

February 1, 2008

Abstract

We report a very detailed relation about the study, by a constrained Monte Carlo dynamic of a 4D EA spin glass model ($J = \pm 1$). In particular we concentrate our attention on the study of the behaviour of the system under different dynamical parameters in order to optimize our analysis and try to understand the low energy states structure. We find that in the thermodynamic limit this structure assumes just ultrametric features as already established for the SK model in the SRSB (Spontaneous Replica Simmetry Breaking) theory.

Introduction

At present there are two different and contrasting approaches about the description of the spin-glass phase of a finite-dimensional EA model. The first, the replica approach, follows the solutions of the SK model describing the nature of spin-glass phase at finite dimensions similar to the one of the mean-field theory [18]. The second approach is based on the phenomenological

1

theory of droplets and predicts a spin-glass phase dominated by only one equilibrium state [13]. The difficulties in the research of analytic results in this field imposes that a large part of the work is delegated to the numerical simulations. A large number of works ([19][10][12][7]) supports the replica approach which at present seems the more appropriate for the description of realistic spin-glasses.

In this work we study the four-dimensional Ising Spin Glass at zero external magnetic field by means of Monte Carlo numerical simulations for several small sizes $N = L^4$ with L=3, 4, 5, 6, 7, 8 with coupling quenched $\pm J$.

In detail we will concentrate our attention on the structure of low energy states of the model by a constrained dynamic that will be here examined very in detail (see also [1]). In the first and second section we will briefly mention the analytic results obtained with the SK model and we will add some comments about the main numerical works undertaken about the ultrametric problem in spin-glasses (see also [9]). In section 3, we will introduce the metric used for this model. Sections 4, 5, and 6 are dedicated to the description of the simulated system and to the Monte Carlo constrained dynamic realized. Finally the last sections report the results of the numerous simulations effected.

1 The ultrametricity in the mean field theory

Rigorous analytic studies ([18][3][8]) have clearly demonstrated the ultrametric structure of low energy states of the SK model. The starting point of this analysis is the calculation of the probability for three pure states $\alpha_1, \alpha_2, \alpha_3$ to have mutual overlaps

$$q_1 = q^{\alpha_2 \alpha_3}, \ q_2 = q^{\alpha_3 \alpha_1}, \ q_3 = q^{\alpha_1 \alpha_2} \ . \tag{1}$$

One can demonstrate [3] that subsists the relation

$$P(q_1, q_2, q_3) = \tfrac{1}{2} P(q_1) x(q_1) \delta(q_1 - q_2) \delta(q_1 - q_3) +$$

$$+ \frac{1}{2} \{ P(q_1) P(q_2) \theta(q_1 - q_2) \delta(q_2 - q_3) + 2 \text{ permutations} \} \ . \tag{2}$$

The study of this equation [3] tells us that $P(q_1, q_2, q_3)$ is null except when two of the overlaps are equals and not larger of the third one. If we define

the distance between two pure states as

$$d^2_{\alpha\beta} = \frac{1}{N} \sum_i (m_i^\alpha - m_i^\beta)^2 \ , \tag{3}$$

(this is not the only way), can be easily verified that

$$d^2_{\alpha\beta} = 2(q_{EA} - q_{\alpha\beta}) \ . \tag{4}$$

In this contest the equation (2) establishes that triangles builded with three configurations, chosen in agreement with their Boltzmann weights, are always either equilaters or isosceles, and in this last case the different side is the smallest. In this prospective, we need to replace the triangular inequality

$$d_{ab} \leq d_{ac} + d_{bc} \tag{5}$$

with the more restrictive condition

$$d_{ab} \leq max(d_{ac}, d_{bc}) \ . \tag{6}$$

A space with this metric is called **ultrametric**.

2 Ultramericity in literature

Attempts of analysis with calculator of ultrametric properties of finite dimensional spin glasses are very few in literature ([15][12]) and have not given any decisive contribute. The more remarkable results of interest for our work are probably those obtained by Ciria, Parisi and Ritort [12] in 4 dimensions at T=1.4. Now we discuss the crucial elements of the philosophy followed in that work. For every triad of three overlaps that one can build (see also section 4) from three different replicas of the system (with the same disorder realization but an autonomous dynamic) one analyses, for a fixed bigger overlap in an established range of values, the difference between the middle overlap and the smallest excluding terms where the triangular inequality is violated from finite size corrections. For this purpose one defines for every overlap a distance

$$d_{\alpha\beta} = [2(q_{max} - q^{\alpha\beta})]^{1/2} \ , \tag{7}$$

where q_{max} is the largest overlap relative to the thermodynamic limit

$$q_{max} = \lim_{L \to \infty} q_{max}^L \ , \tag{8}$$

(which can be obtained by the scaling relation $P(q > q_{max}) \sim P_{max} \mathcal{F}(\mathcal{N}(\mathrm{II} - \mathrm{II}_{\Updownarrow\dashv\S})^{\frac{\mathcal{D}}{\lceil \mathrm{II}}})[12]$), and one consider only the overlap triads that satisfy the inequality

$$d_{max} \leq d_{min} + d_{middle} \ . \tag{9}$$

The results of this analysis have not given a decisive answer to the problem. In effect if we observe figure (1), where is indicated in abscissas the value of $\delta q = q_{medio} - q_{min}$ and in ordinates $P(\delta q)$, we note that a dependence on the curves from the volume is not determined with sufficient statistic precision. By these simulation people thought that it were possible to increase the volume size to obtain a precise indication of a ultrametric behaviour in the infinite volume limit. Similar works about the SK model [16][17] have given very satisfying results pointing out clearly the ultrametric structure of the states. The first of these works is from Bhatt Young [16]. The result is shown in figure (2). In this case the curve tends explicitly to narrow increasing the lattice volume showing the existence of the predicted structure between the states.

3   The distance

There are two big problems for a direct analysis of the ultrametric structure:
    1) There are corrections for small N that are not known analytically
    2) The triangular inequality can impose some bonds that are not easily distinguishable from the more restrictive ones provided from the ultrametric inequality.
    To understand the last affirmation we take a triangle with sides d_1, d_2, d_3 and let d_3 the smallest one. The triangular inequality imposes that

$$|d_2 - d_3| \leq d_1 \leq d_2 + d_3 \tag{10}$$

to compare with the ultrametric request

$$d_1 = d_2 \ . \tag{11}$$

A correction due to the limited value of N causes some violations in the last equation

$$d_1 = d_2 \pm O(1/N^\delta) \ . \tag{12}$$

If d_3 is fairly little, the imposed conditions from the two inequality are practically indistinguishable. To get over these problems it is necessary to define a metric which makes the two conditions as distinct as possible.

We define (see also [1]) the square distance between the two pure states with overlap q as

$$d^2 = \frac{q_{EA} - q}{2q_{EA}} \ , \tag{13}$$

so when $q = -q_{EA}$ we will have $d^2 = 1$, the lowest overlap imposes a largest square distance, while for $q = q_{EA}$ we have that $d^2 = 0$, the largest overlap involves a lowest square distance. The triangular inequality imposes that when we take three pure states the mutual distances satisfy the relation

$$d_{13} + d_{23} \geq d_{12} \ . \tag{14}$$

Squaring both members we have

$$(d_{13} + d_{23})^2 \geq d_{12}^2 \tag{15}$$

and so

$$\frac{(q_{EA} - q_{13})}{2q_{EA}} + \frac{(q_{EA} - q_{23})}{2q_{EA}} + 2\frac{\sqrt{q_{EA} - q_{13}}\sqrt{q_{EA} - q_{23}}}{2q_{EA}} \geq \frac{q_{EA} - q_{12}}{2q_{EA}} \ . \tag{16}$$

We fix now two of the three overlaps, for exemple

$$q_{13} = q_{23} \equiv q^{fix} \tag{17}$$

(we take for convenience of notation $d_{12} \equiv d$ and $q_{12} \equiv q$).
From the equation (15) we have

$$4(q_{EA} - q^{fix}) \geq q_{EA} - q \geq 0 \ , \tag{18}$$

because when $d_{13} \geq d_{23}$ then the triangular inequality imposes

$$d_{12} \geq (d_{13} - d_{23}) \ . \tag{19}$$

5

In this way the overlap q (the observable we will study in our Monte Carlo simulations) is forced from the triangular inequality to satisfy the relation

$$q_{EA} \geq q \geq 4q^{fix} - 3q_{EA} \ . \tag{20}$$

It is reasonable to choose for our simulations for exemple

$$q^{fix} = \frac{2}{5}q_{EA} \ . \tag{21}$$

With these conditions the triangular inequality imposes that

$$-\frac{7}{5}q_{EA} \leq q \leq q_{EA} \ (\text{DT bound}) \ , \tag{22}$$

while the ultrametric one imposes

$$\frac{2}{5}q_{EA} \leq q \leq q_{EA} \ (\text{UM bound}) \ . \tag{23}$$

Now the difference between these two situations is evident. When N is limited (and little) these inequalities will be violated. The possible ultrametric structure will completely manifest itself only in the limit of infinite volume. We will try to understand if the more we increase the lattice size the better the ultrametric bound is satisfied.

We will use for q_{EA} the thermodynamic limit calculated in a work of Ciria, Parisi and Ritort [12]; at $T = 1.4$, $q_{EA} = .54$. So we will take for our simulations

$$q^{fix} \simeq .21 \tag{24}$$

4   The model

The studied model in this work is a Ising Spin Glass in four dimensions in absence of external magnetic field. It is defined within a 4D lattice, where the lattice sites are individualized from the integer values of the fourdimensional vector i. In every site is defined a Ising spin ($\sigma_i = \pm 1$). The couplings $J_{i,j}$ are distributed in binary way

$$P(J_{i,j}) = \frac{1}{2}\delta(J_{i,j} - 1) + \frac{1}{2}\delta(J_{i,j} + 1) \tag{25}$$

so that they assume the values $J_{i,j} = \pm 1$ with the same probability and their action range is limited to only first neighbouring spins. The hamiltonian of the system is

$$H[\sigma] \equiv -\frac{1}{2} \sum_{i,j} J_{i,j} \sigma_i \sigma_j \ . \tag{26}$$

From these definitions, if we consider the overlap between two thermalized replicas of the system

$$Q = \frac{1}{N} \sum_{i=1}^{N} \rho_i \sigma_i \qquad , \tag{27}$$

it is possible to calculate easily the overlaps distribution function

$$P(q) = \overline{P_J(q)} = \overline{\left\langle \delta(q - \frac{1}{N} \sum_{i=1}^{N} \rho_i \sigma_i) \right\rangle} \tag{28}$$

which is the observable upon which we will concentrate our attention.

5   The dynamic

The exploration of the phase space at a particular temperature (T=1.4 in our case) is directed principally by two algorhythms
  • Monte Carlo Algorhythm
  • Bound Algorhythm
    The Monte Carlo Algorhythm used in our simulations generates a single-spin-flip Glauber dynamic, while the Bound Algorhythm, the very heart of the simulations, acts re-examining the Monte Carlo flips on the ground of a bound imposed on the overlaps. They work in this way: One takes three replicas of the system, S_1, S_2, S_3, with the same realization of the disorder but different initial spin configurations. One builds the overlaps

$$q_{(12)} = \frac{1}{N} \sum_{i=1}^{N} S_1^i S_2^i \quad q_{(13)} = \frac{1}{N} \sum_{i=1}^{N} S_1^i S_3^i \quad q_{(23)} = \frac{1}{N} \sum_{i=1}^{N} S_2^i S_3^i \tag{29}$$

and fixes the value of $q_{(13)}$ and $q_{(23)}$ equal to q^{fix} (as before establisched) and defines the tolerance parameter inside of which one consents same fluctuations

$$q_{(13)} = q_{(23)} = [q^{fix} \pm \varepsilon] \ . \tag{30}$$

The spin changes proposed from the Monte Carlo Algorhythm that satisfy this request will be accepted. The others will be rejected.

Now see in detail how to operate the chosen. Suppose that in a particular instant at a particular site i the Monte Carlo Algorhythm proposes to the Bound Algorhythm the spin changes

$$S_1^i \to \tilde{S}_1^i \quad S_2^i \to \tilde{S}_2^i \quad S_3^i \to \tilde{S}_3^i . \tag{31}$$

Let be $q_{(13)}^V = \frac{1}{N}\sum_{i=1}^N S_1^i S_3^i$ and $q_{(23)}^V = \frac{1}{N}\sum_{i=1}^N S_2^i S_3^i$ the overlaps calculated from the previous accepted configurations. Consider to begin the spin change $S_1^i \to \tilde{S}_1^i$. One calculates the product $q_{13}^i{}' \equiv \tilde{S}_1^i S_3^i$ and tries to replace $q_{13}^i \equiv S_1^i S_3^i$ with $q_{13}^i{}'$ in $q_{(13)}^V$

$$q_{(13)}^{test} \equiv q_{(13)}^V - q_{13}^i + q_{13}^i{}'. \tag{32}$$

Only in the case in which $q_{(13)}^{test} \in [q^{fix}-\varepsilon, q^{fix}+\varepsilon]$ we accept the configuration $\tilde{S}_1^i$.

Consider now the spin change $S_2^i \to \tilde{S}_2^i$ and one imposes an argument similar to the previous for the overlap $q_{(23)}^V$. Also in this case we accept the change only if $q_{(23)}^{test} \in [q^{fix} - \varepsilon, q^{fix} + \varepsilon]$.

One examines to finish the spin change $S_3^i \to \tilde{S}_3^i$. We calculate $q_{13}^i{}'' \equiv \tilde{S}_3^i S_1^i$ e $q_{23}^i{}'' \equiv \tilde{S}_3^i S_2^i$ and replace q_{13}^i with $q_{13}^i{}''$ in $q_{(13)}^V$ and q_{23}^i with $q_{23}^i{}''$ in $q_{(23)}^V$

$$q_{(13)}^{test} \equiv q_{(13)}^V - q_{13}^i + q_{13}^i{}'' \tag{33}$$

$$q_{(23)}^{test} \equiv q_{(23)}^V - q_{23}^i + q_{23}^i{}'' . \tag{34}$$

Only if both of them will be included in the defined interval we will accept the replacement $S_3^i \to \tilde{S}_3^i$.

For our simulations we have established after several tests that the better value of the tolerance parameter is $\varepsilon = 0.04$ (see section 9).

6 Initial configurations

The initial spins configurations are so arranged (it is not the only possible way) :

1) One generates in a random way the spin configuration of the replica S_1.
2) One builds the replica S_3 so that 60% of spins are (chosen in a random way) equals to the correspondent spins of the replica S_1 and the others are opposites.
3) The replica S_2 will be builded in a way such that 40% of spins (chosen casually) are opposites to those correspondent of the replica S_3 and the others are equals.

These choices allow to begin the simulations in a random spin situation and from values of constrained overlaps

$$q_{(23)} = q_{(13)} \simeq 0.2 \ . \tag{35}$$

$q_{(12)}$ varies with the statistic shows in figure (3).

7 Free and constrained P(q)

The first part of this work regards the study of the overlaps distribution P(q) at the temperature T=1.4. This work is useful for two aims. The first is to find some good annealing schedules for all lattice sizes (taken successively as foundation for the study of the ultrametricity) while the second regards the understanding of the behaviour of this distribution for $q \simeq 0$, that is to say P(0). The analysis we have done confirms the results already obtained in other works [12][14]; it seems that there is a clean indipendence of P(0) from the size of system in agree with the Parisi's theory. This situation seems to confirm the existence of a large number of pure states in the glass-phase that are describable with the theory of SRSB (Spontaneous Replica Symmetry Breaking). In the figure (4) we report the results of these simulations. For lattices of size L=3 and L=4 the averages over the disorder are effected with 1200 different realizations, for L=5 with 700 samples and for the lattice of size L=6 we have averaged with 350 samples.

As already described in detail, the study of the ultrametricity are made with a constrained dynamic. We have fixed two of three overlaps built with three replicas of the system and we have observed the behaviour of the not constrained one changing the lattice size. The triangular inequality , considering the bounds imposed to the dynamic, tell us that

$$-\frac{7}{5}q_{EA} \leq q \leq q_{EA} \ \text{(DT bound)} \tag{36}$$

while the ultrametric one

$$\frac{2}{5}q_{EA} \le q \le q_{EA} \text{ (UM bound)} \qquad (37)$$

(q_{EA}=0.54). For finite (and little) N these inequalities will be violated. A possible ultrametric structure will reveal oneself completely only in the thermodynamic limit. The annealing schedule used for these simulations contains larger numbers of Monte Carlo Steps compared with the ones used for the free P(q) thermalization. Not only the number of MCS is on average larger that the previous case, but for sizes L=5, L=6, L=7 and L=8, the step of the simulated annealing is reduced to one half. Of course the last operation caused a greater precision in the research of the equilibrium, but so the simulation times are resulted clearly longer. This choice (extremely prudent) is operated because, cause the originality of the dynamic, it is not still defined any thermalization method (however the annealing schedule relative to the thermalization of the free P(q) would be more than enough to assure the equilibrium of our system).

Figure (5) shows the result of simulations [1] varying of the lattice size.

The behaviour of this curves point out a clear dependence of constrained P(q) from the volume of system. Increasing the lattice side we observe that the function tends to assume such a shape that the ultrametric bound is more and more satisfied. Figure (5) shows, with vertical lines, both triangular bound and

$$-0.75 \le q \le 0.54 \quad \text{(DT bound)} , \qquad (38)$$

ultrametric one

$$0.21 \le q \le 0.54 \quad \text{(UM bound)}. \qquad (39)$$

It can be observed that increasing lattice volume there is a systematic shift of the peak toward overlap values consented from the ultrametric bound. Similar remarks can be made about tails relative to negative overlaps because they too tend toward values indicated from vertical continuous lines. So it is possible to deduce a clear tendency for large volumes to a fully ultrametric behaviour of the system. The study of the variation of the largest overlap (q^L_{max}) with the lattice size [1] (see figure (5) consents moreover to establish a limit to the peak shift of constrained P(q). Best fits made with the function

$$q_{max}^L = q_{max}^\infty + \frac{\alpha}{L^\gamma} \qquad (40)$$

indicate that $q_{max}^\infty = 0.31 \pm 0.09$. It is to say that in the thermodynamic limit the constrained P(q) will assume her largest value just inside the ultrametric bound.

Further confirmation of the ultrametric behaviour of the system can be seen studying the variation of integral (see also [1])

$$I_L = \int_{-1}^{0.21} P_L(q_L)(q_L - 0.21)^2 dq_L +$$

$$+ \int_{0.54}^{1} P_L(q_L)(q_L - 0.54)^2 dq_L \qquad (41)$$

As figure (6) shows this tends to zero in the thermodynamic limit as expected.

8   Thermalization

It is very important in a computer simulation to be sure that obtained results describe the equilibrium system fluctuations. The main problem in the research of this condition is that generally we are interested to the low temperature behaviour of the system where the phase space is very complex. Theorically we should make simulations for a infinite time to be sure that equilibrium is joined but this is obviously impraticable. We so make everytime errors whit finite-time simulations, but it is possible to prove that these ones are comparables with statistical fluctuations. R.N. Bhatt and A.P. Young [11] suggested a thermalization criterion that is so resumable:

For every disorder realization one define two overlaps

$$Q(t) = \frac{1}{N} \sum_i S_i(t_0) S_i(t_0 + t) \qquad (42)$$

and

$$Q'(t) = \frac{1}{N} \sum_i S_i^{(1)}(t_0 + t) S_i^{(2)}(t_0 + t) \ . \qquad (43)$$

Where t_0 is the esteemed equilibrium time. In the $t \to \infty$ limit the two overlaps have the same distribution, but also in a finite-time observation (inside an error margin) they are convergent.

For small times $Q(t)$ assumes values very near to 1 and the P(q) function will have a peak just there. In the same situation $Q'(t)$ will have (starting from a random spin distribution) a Gaussian shape peaked around zero and with amplitude $N^{-\frac{1}{2}}$. When we increase t, $Q(t)$ and $Q'(t)$ tend to the same distribution. We can say to be in equilibrium when Monte carlo statistical errors are bigger than finite-time simulation errors. In other words when the two overlap distributions are the same function unless statistical errors. We report in figure (8) results of this method applied to the lattice with size L=3 at the temperature T=1.4 (everytime we use $\tau_0 = t_0$).

Considered the originality of dynamic applied in these simulations (we have three replicas of the system and so we can't use the Bhatt-Young method) , a criterion of thermalization has not yet been defined. However, we think that a further confirmation (thermalizing the free P(q) we have equilibrium in all phase space and in particular in the small part we are studying with our dynamic) of the joined equilibrium for our system comes from the study of the constrained P(q) for different and successive MCS. Specifically, the test we made consists in the control, for a given annealing schedule, of the behaviour of the distribution function with respectively the first third, the second third and the last third of MCS used for the calculation of statistical averages. The result relative to size L=5 with 100 samples is shown in figure (9). It can be observed that the three curves are pratically identical. In fact oscillations between the functions are well inside the errors from which are afflicted. This test, made on all lattice size, has given, with our annealing schedule, good results comforting ourself about the joined equilibrium of the system. This is not obviously the faster method (we are trying to find something better) but it is sure and for now this is enough.

9   The tolerance parameter ε

We have used a particular attention to the behaviour of the constrained P(q) varying the tolerance parameter. We have concentred our study in the lattice of size L=3 and L=5 performing a lot of simulations in order to understand the develop of the overlaps distribution function under the imposition of more and more restrictive bounds.

The work on the lattice of size L=3 is effectued with a small statistic but a large range of tolerance parameter values, vice versa for the lattice of size

L=5 we have used a robust statistic but a little number of ε. The two results obtained are just compatibles and show, see figures (10)(11), a continuous shifting of the tail relative to the negative overlaps towards values more and more near to that imposed from the ultrametric bound. This observation suggest us to choice the smallest possible tolerance parameter. There is obviously some restrictions. Too small tolerance parameter values would impose too restrictive bounds in the simulation of the lattice L=3 while too big values could be not enough to force the distribution in a decisive way. Moreover when the tolerance parameter is bigger than $1 + 2/5q_{EA}$ we refind the free overlaps distribution (see figure (4)) and all dynamical spin-flips are accepted from the bound algorhythm. When ε decrease the number of spin-flips accepted begin smaller and to have enough statistic we must increase the number of MCS for every sample. So we also have to choose ε so that calculator simulations are not too long in time. After long tests we have established that best compromise in our case is $\varepsilon = 0.04$.

10 The constrained P(q) 2^a part

The evidence of first results lead us to deepen the feature of the ultrametric structure in the examined system. So we further modify the dynamic without changing the philosophy of the approach. Now we fix the overlap q_{23} and q_{13} to different values (in the first part of the work we fixed $q_{13} = q_{23} \simeq \frac{2}{5}q_{EA}$). In particular we made our simulations with

$$q_{23} \simeq \frac{4}{5}q_{EA} \qquad q_{13} \simeq \frac{1}{5}q_{EA} \tag{44}$$

or better $q_{23} = 0.43$ and $q_{13} = 0.10$. By this modification we expect, differently from the previous case, that increasing the size of the lattice the third overlap q_{12} (following the same notation defined in section 5, $q_{12} = Q$) assumes exclusively the value $q = q_{13}$ how imposed from the ultrametric bound so that the constrained distribution function of the overlaps tends to a Dirac Delta function peaked around q_{13}.

   The results of these simulations (see also [1]) are shown in figure (12). It is evident in this case a development of the overlaps distribution function very singular. There is a systematic shift, starting from small volumes, either of the peak of bigger tallness or the smaller peak toward, probably, the overlap

of value $q_{13} = 0.10$. One can see moreover that increasing the lattice size the curve tends to narrow and the smaller peak is "absorbed" in the tail of the predominant one so that the distribution function assumes the expected shape.

The study of the biggest overlaps develop with the lattice size (see figure (13)) consents to establish a limit to the shift of the predominant peak of constrained P(q). Our best fits with the function

$$q_{max}^L = q_{max}^\infty + \frac{\alpha}{L^\gamma} \tag{45}$$

affirm that $q_{max}^\infty = 0.100 \pm 0.028$. So in the infinite size limit our function will tend to settle about a value compatible with q_{13}.

To understand at last which is the shape that the constrained P(q) assumes in the thermodynamic limit we have effected a study of variation of the integral

$$I_L = \int_{-1}^{1} P_L(q_L)(q_L - 0.10)^2 dq_L \tag{46}$$

with the lattice size. Best fits (see figure (14)), always executed by the function

$$I_L = I^\infty + \frac{\alpha}{L^\gamma} \ , \tag{47}$$

indicate that

$$I^\infty = \lim_{L \to \infty} I_L = 0.000 \pm 0.002 \ , \tag{48}$$

so in the thermodynamic limit the integral (46) will be zero. In other words, being

$$P_L(q_L)(q_L - 0.10)^2 \geq 0 \tag{49}$$

also

$$I_L \geq 0 \qquad \forall L \ , \tag{50}$$

and in order to satisfy the (48) must be verified that

$$P(q) = \lim_{L \to \infty} P_L(q_L) = \delta(q_L - 0.10) \tag{51}$$

as required from the ultrametric hypothesis about the states structure.

11 Another way to see ultrametric structure

Another approach we tried to verify the existence of a possible ultrametric structure between the low energy states of a realistic spin glasses is suggested from the work [17] about the hipercubic lattice .

We take three replicas S_1, S_2, S_3 of the system with the same disorder realization and build the overlaps q_{12}, q_{13}, q_{23}.

In the previous works we fixed by constrained dynamic the value of two of three overlaps (at the same Q^{fix} or at differents Q^{fix}) and observe the behaviour of the third one.

Now we define an overlaps bound, say $[q_{fix1}, q_{fix2}]$ (with $q_{fix1} \geq q_{fix2}$), and then check (with a not constrained dynamic) whether the largest overlap falls inside the established bound. In this case we calculate the difference between the other ones $\delta q = q_{mid} - q_{min}$ and plot the distribution function $P(\delta_q)$. We aspect to obtain in the termodynamic limit a Dirac delta function peaked around zero.

We have chosen for our simulations the interval $[q_{EA}, 2/5q_{EA}]$ for lattice sizes L=4,6,8 with 400, 200 and 100 samples respectively at the same temperature T=1.4.

As we can see in figure (15) increasing the volume of the lattice the curve tends to narrow more and more showing the presence of a not trivial structure between the low energy states of the model. As well as in the work about hypercubic celles, the behaviour of the curve seems to manifest a ultrametric feature of the system.

Our last simulation with all others developed in this work we lead to suppose that the spontaneous replica symmetric breaking is a good analitic approach for the study of realistics Eduards Anderson Spin Glasses.

Conclusions

In this work we describe in a very detailed way the constrained dynamic used in Monte carlo simulation of a four dimensional Eduards Anderson Ising Spin Glass to understand the nature of the glass phase for these systems. We have concentrated our efforts in the study of the low energy states structure. After having defined a metric (section 3) in the overlaps space, we have effected a long series of simulations (section 7, 8, 9, 10) in 4D lattice of sizes

(L=3,4,5,6,7,8) looking for some confirmations about a possible analogy with the model SK. From the obtained results, it seems to be possible to affirm that a not trivial low energy states structure in the glass phase of a finite dimensional Spin Glass really exists. In particular the results shown in figures (4), (12) and (5) claim the concreteness of the hypothesis proposed by G. Parisi about the origin and the kind of this structure. The origin should be researched in the spontaneous replica symmetry breaking [2][4][5][6] and the kind of the structure really seems to be the ultrametric one as already established for the SK model.

References

[1] **A. Cacciuto, G. Parisi, E. Marinari** cond-matt /9608161 to be published on J. Phys. A;

[2] **G. Parisi**, *Toward a mean field theory for Spin Glasses*, Phys. Lett. 73 A, 203 (1979);

[3] **M. Mezard, G. Parisi, N.Sourlas, G.toulouse, M. Virasoro**, *Replica symmetry breaking and the nature of the spin glass phase*, J.physique 45 (1984) 834-854.;

[4] **G. Parisi**, *A sequence of approximated solutions to the S-K model for spin glasses*, J. Phys A: Math Gen. 13 (1980) L115-L121.;

[5] **G. Parisi**, *The order parameter for spin glasses: A function on the interval 0-1*, J. phys A: Math. Gen, 13 (1980) 1101-1112.;

[6] **G. Parisi**, *Order Parameter for Spin Glass*, Phys. Rev. Lett. 50, No.14 (1983).;

[7] **A. P. Young**, *Direct determination of the Probability Distribution for the Spin-Glas Order Parameter* Phys. Rev. Lett. 51,No.13 (1983);

[8] **M. Mezard and M. A. Virasoro**, *The microstructure of ultrametricity* J. Physique 46 (1985) 1293-1397;

[9] **R. Rammal G. Toulouse M. A. Virasoro**, *Ultrametricity for physicists* Rev. of Mod. Phys. 58 No.3 (1986).;

[10] **D. Badoni, J. C. Ciria, G. Parisi, F. Ritort, J. pech and J.J. Ruiz-Lorenzo**, *Numerical Evidence of a Critical Line in the 4d Ising Spin Glass* Europhys. Lett. 21 (4), pp. 495-499 (1993).;

[11] **R. N. Bhatt and A. P. Young**, *Numerical studies of Ising spin glasses in two, three, and four dimensions* Phys. Rev. B 37, No. 10 (1988)

[12] **J. C. Ciria, G. Parisi and F. Ritort**, *Four-dimensional Ising spin glass: Scaling within the spin-glass phase* J. Phys. A: Math. Gen. 26 (1993) 6721-6745;

[13] **K. H. Fischer and J. A. Hertz**, *Spin Glasses* Cambridge Studies in Magnetism, ZCambridge University Press (1991).;

[14] **F. Ritort**, *Replica symmetry-breaking effects in spin glasses* Philos. Magaz. B 71, No. 4, 515-524 (1995);

[15] **N. Sourlas**, *Three-dimensional Ising spin-glass and mean-field theory* J. Phys. Lettr. 45 (1984) L969-L975;

[16] **R. N. Bhatt and A. P. Young**, J. Magn. Magn. Matter. 54-57, 191 (1986).;

[17] **G. Parisi, F. Ritort and J. M. Rubí** *Numerical results on a hyper-cubic cell spin glass model* J. Phys. A: math. Gen. 24 (1991) 5307-5320.;

[18] **G. Parisi, M. Mezard and M. A. Virasoro**, *Spin Glass Theory and beyond* World Scientific (Singapore, 1987).;

[19] **E. Marinari, G. Parisi, F. Ritort**, *On the 3d Ising Spin Glass* J. Phys. A: 27, 2687 (1994).;
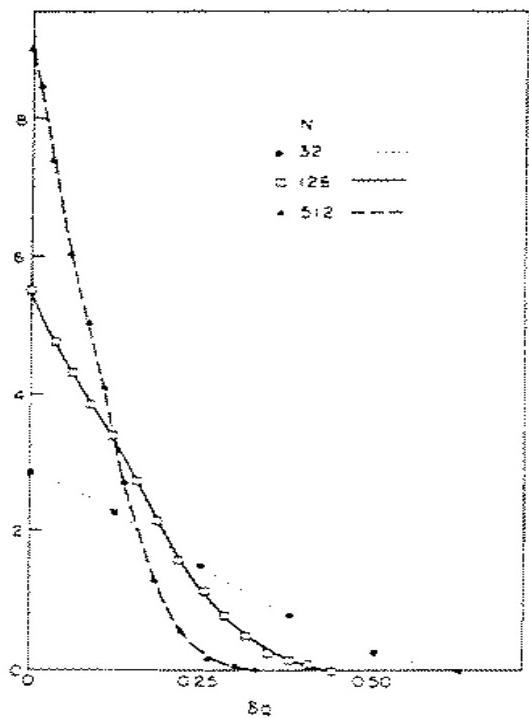
Figure 1: Probability distribution of the difference between the two smaller overlaps ($\delta q = q_{mid} - q_{min}$) when the bigger overlap is smaller than 0.4 from q_{EA} in a four dimensional Ising Spin Glass for different lattice sizes [12]
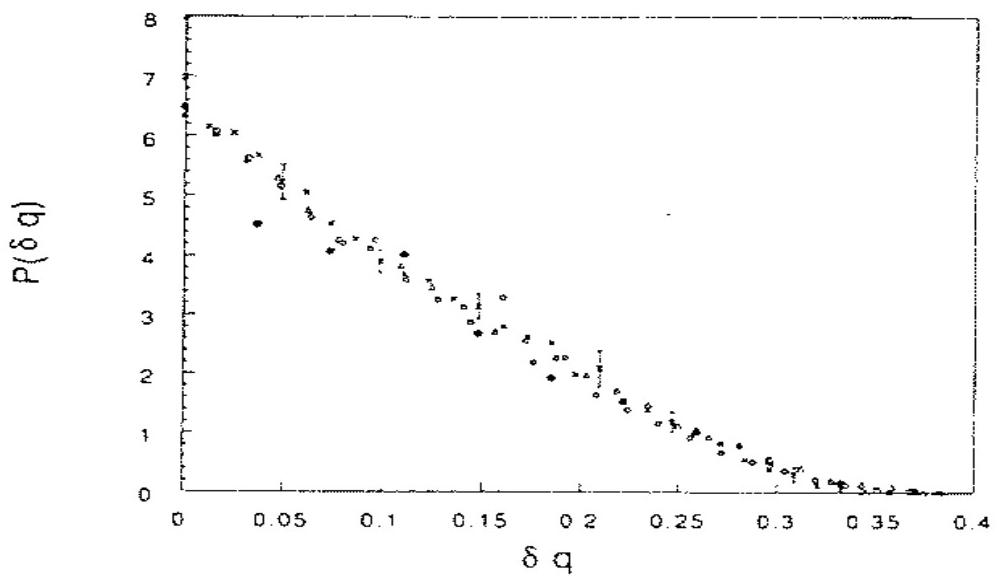
Figure 2: Probability distribution of the difference between the two smaller overlaps ($\delta q = q_{mid} - q_{min}$) for a fixed larger overlap value q=0.5. The temperature is $0.6T_{crit.}$. In the $N \to \infty$ limit, the distribution is expected to become a δ function at the origin [11]
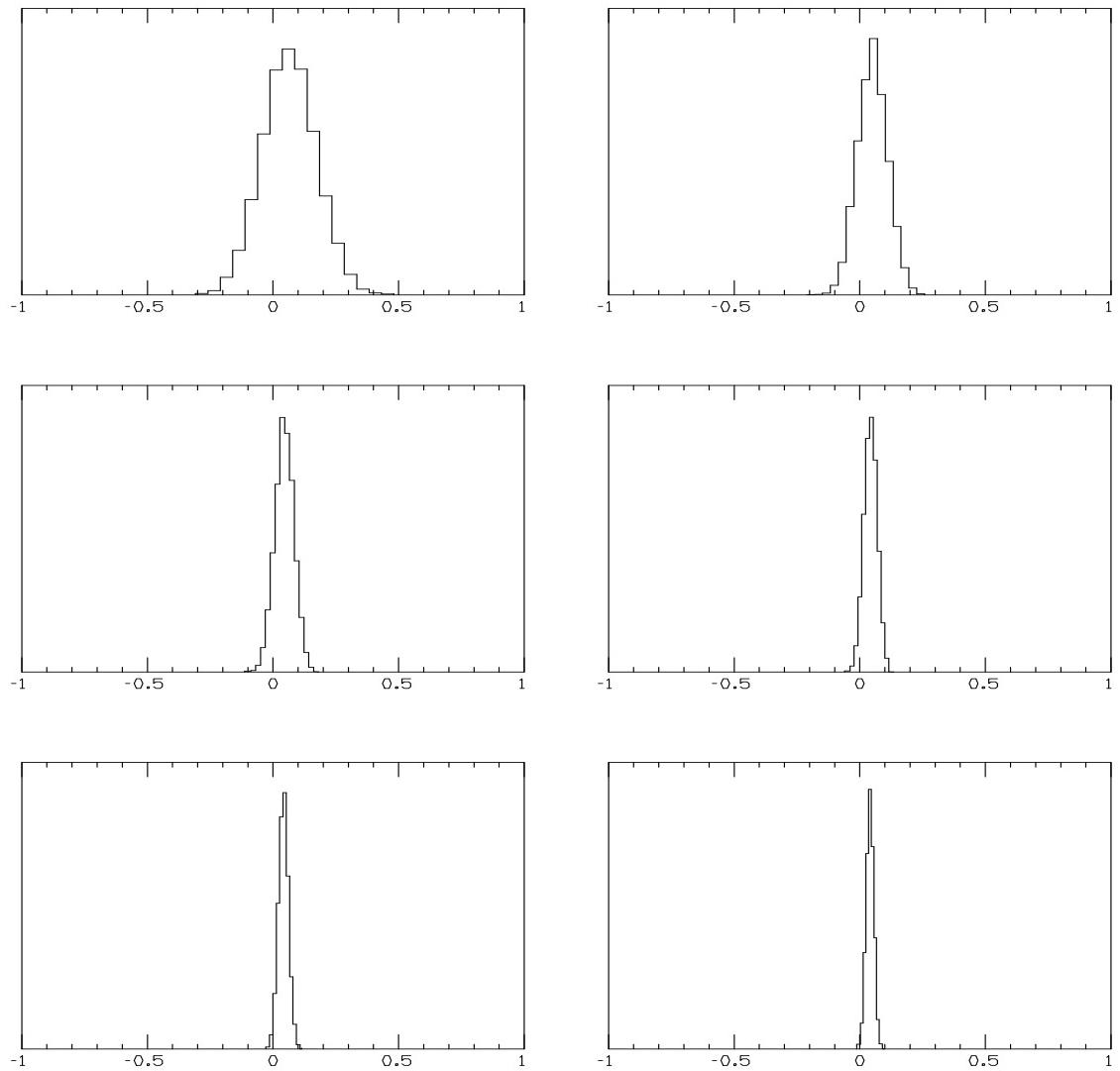
Figure 3: Distribution probability P(q_{12}) (in y-axes) of starting values that $q_{(12)}$ (in x-axes) assumes varying the initial spin configurations with 10000 different starts for sides L=3, 4, 5, 6, 7, 8 in reading order
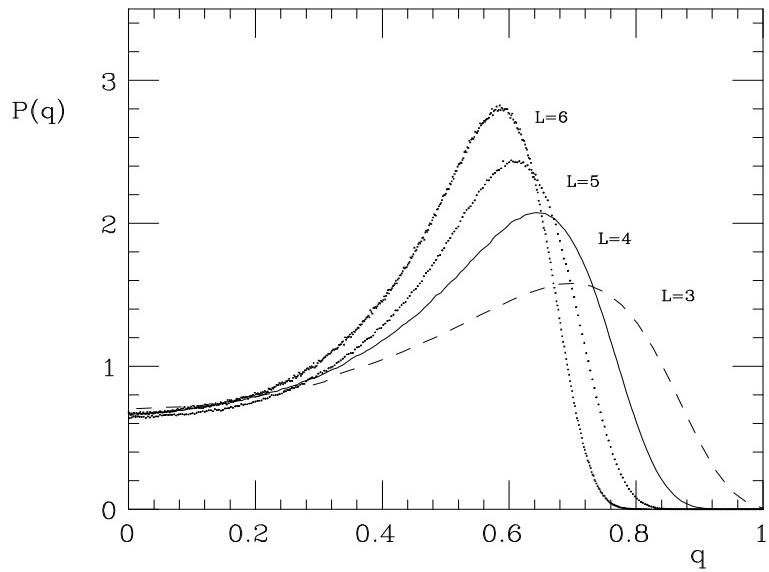
Figure 4: Distribution probability of the overlaps P(q) at T=1.4 for different sizes of the lattice L=3, 4, 5, 6
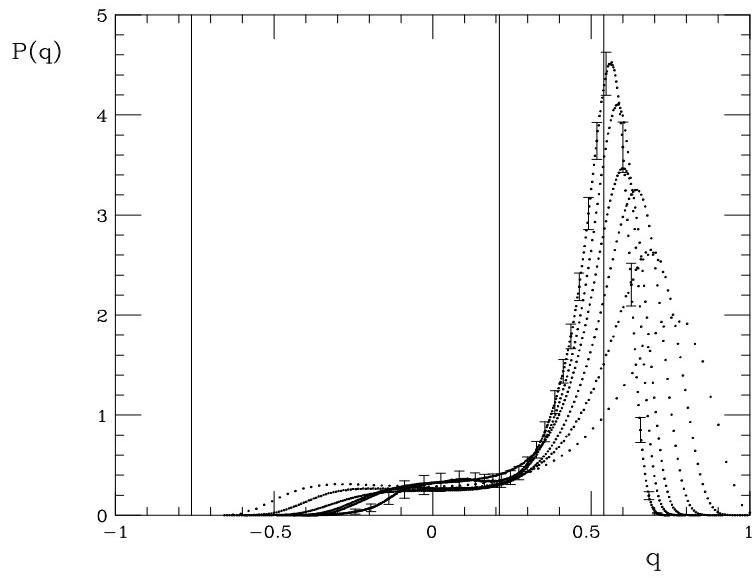
Figure 5: Evolution of the probability distribution of overlaps P(q) with a constrained dynamic a T=1.4 for lattice size L=3, 4, 5, 6, 7, 8.

22
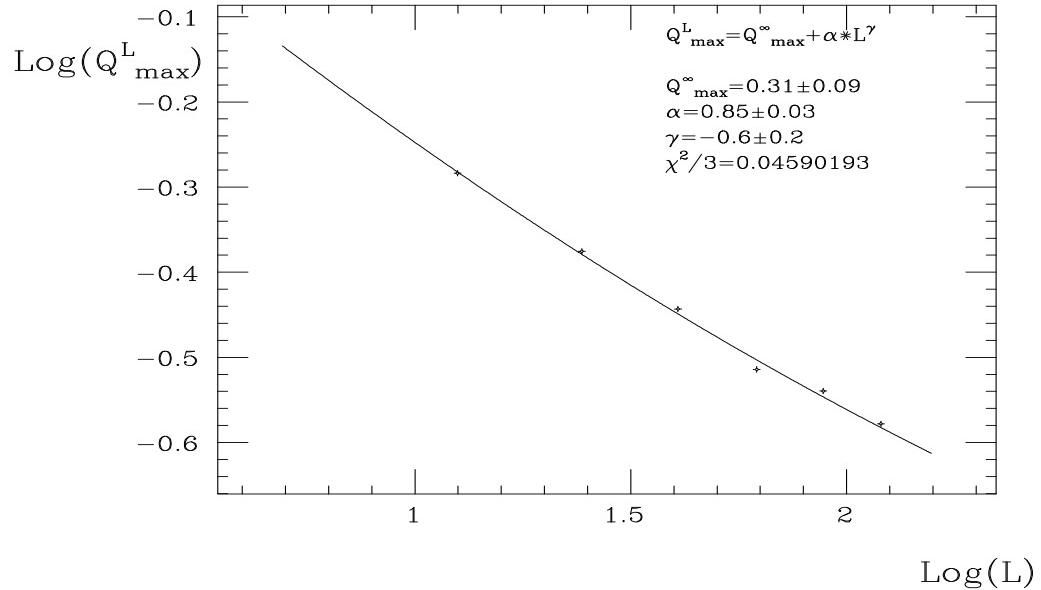
Figure 6: Fit of biggest overlaps for the constrained P(q) with the lattice size by the function $I_{max}^L = I_{max}^\infty + \frac{\alpha}{L^\gamma}$ in log-log scale
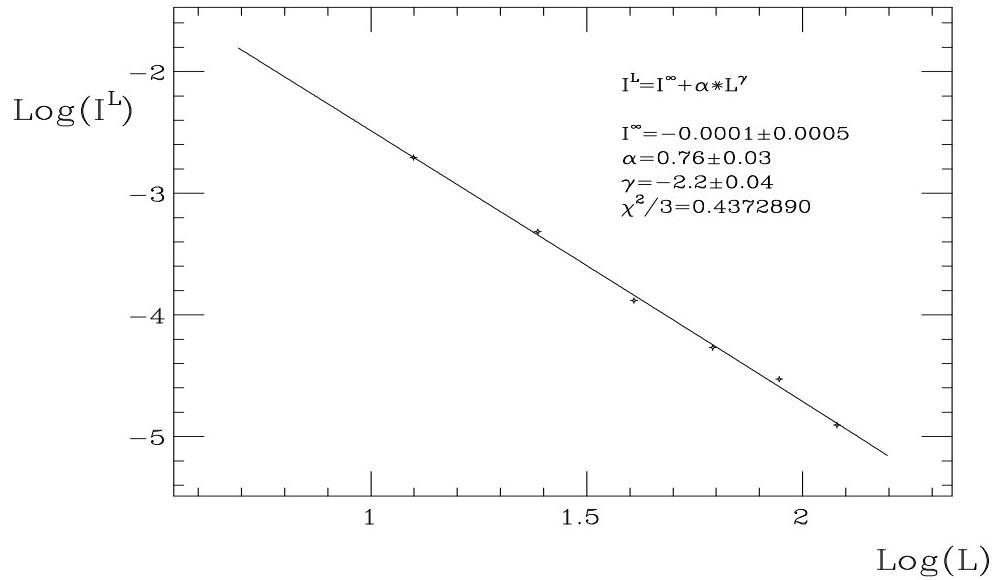
Figure 7: Evolution of the integral $I_L = \int_{-1}^{0.21} P_L(q_L)(q_L - 0.21)^2 dq_L + \int_{0.54}^{1} P_L(q_L)(q_L - 0.54)^2 dq(L)$ with the lattice size in log-log scale

23
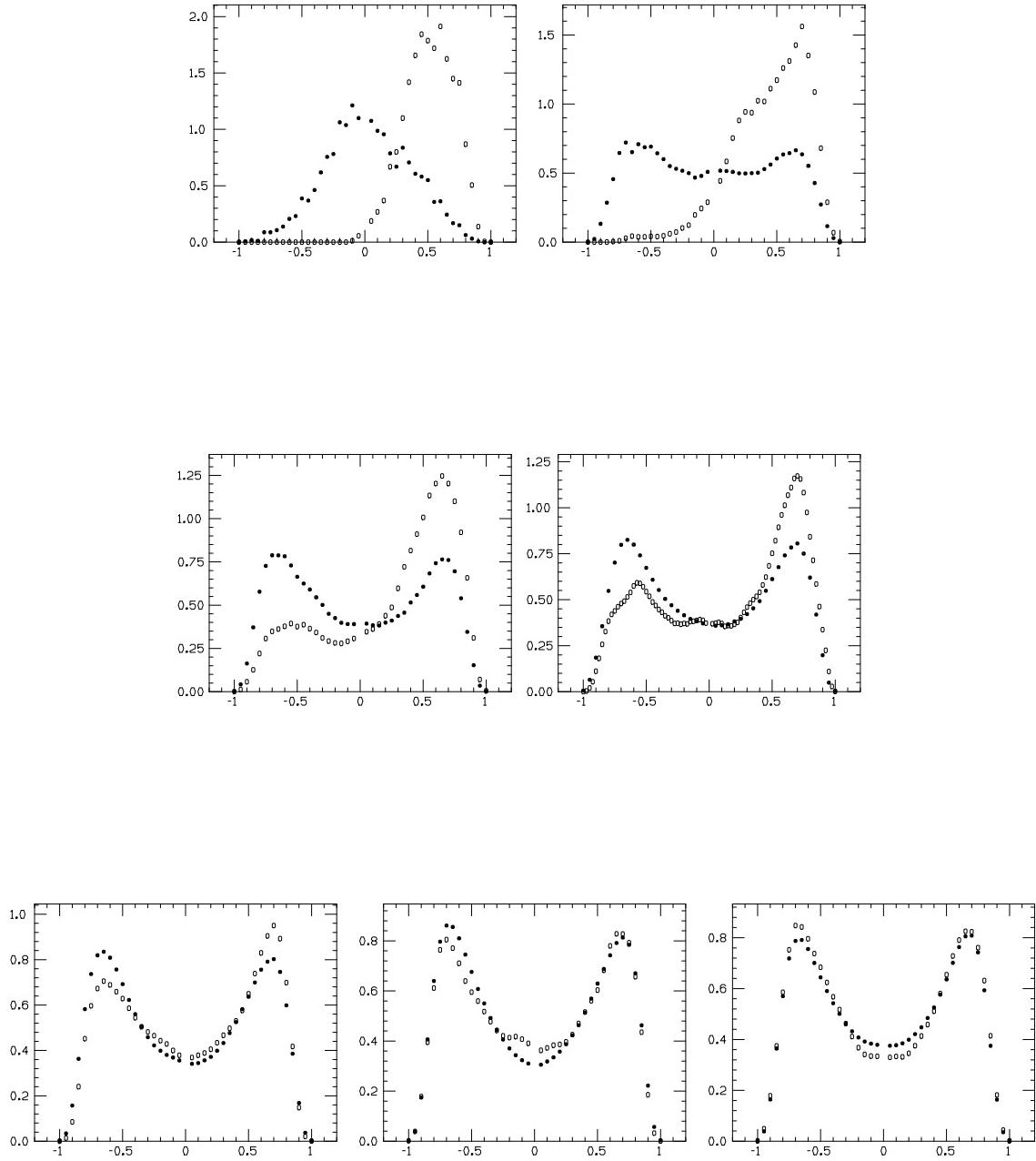
Figure 8: Evolution of free overlap distributions P(q) and P(q') (in y-axes) (see section 8) as a function of thermalization steps (in x-axes). $t_0 = 10, 10^2, 10^3, 10^4, 2 \cdot 10^4, 3 \cdot 10^4, 5 \cdot 10^4$ in reading order
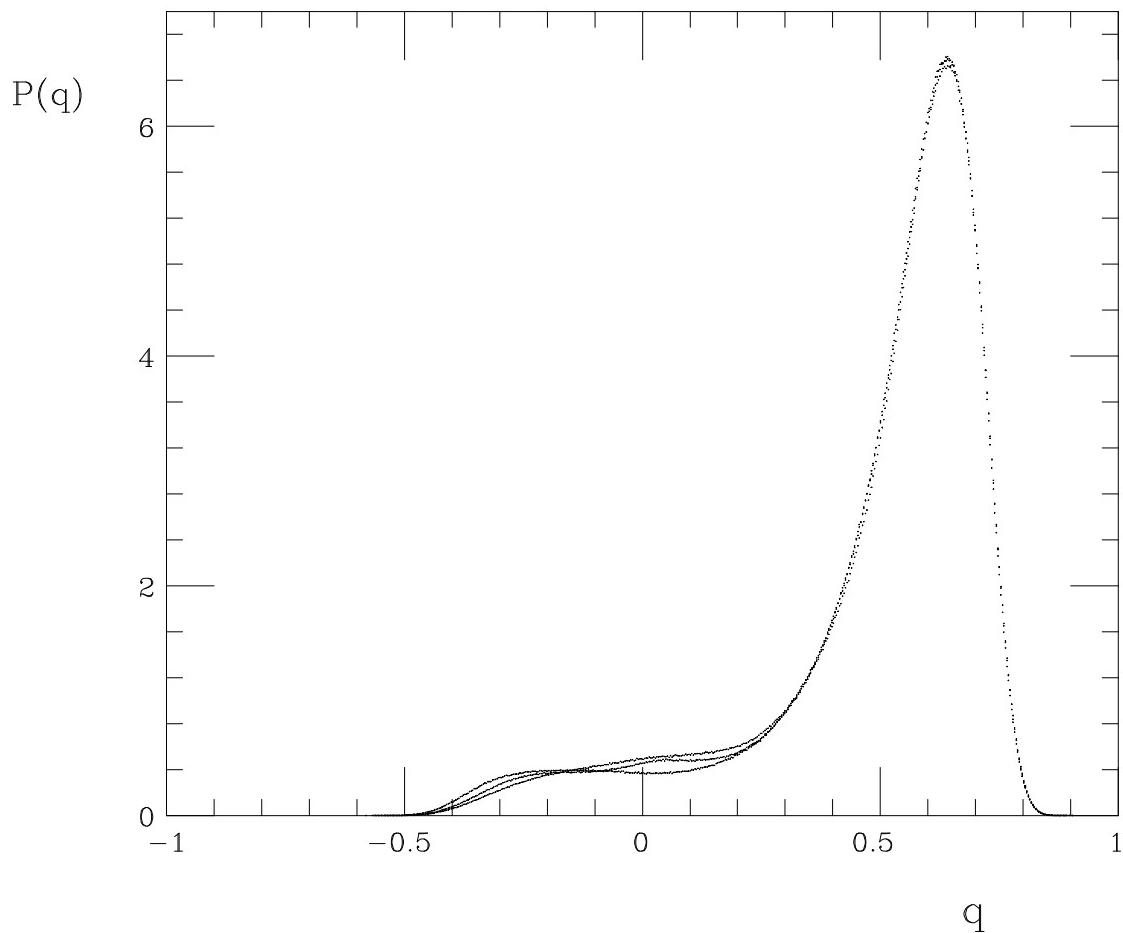
Figure 9: The tree curves (basically coinciding in the plot) are for constrained P(q) in the first, the second and the third of the run after the annealing scheme described in the text), L=5, 100 samples
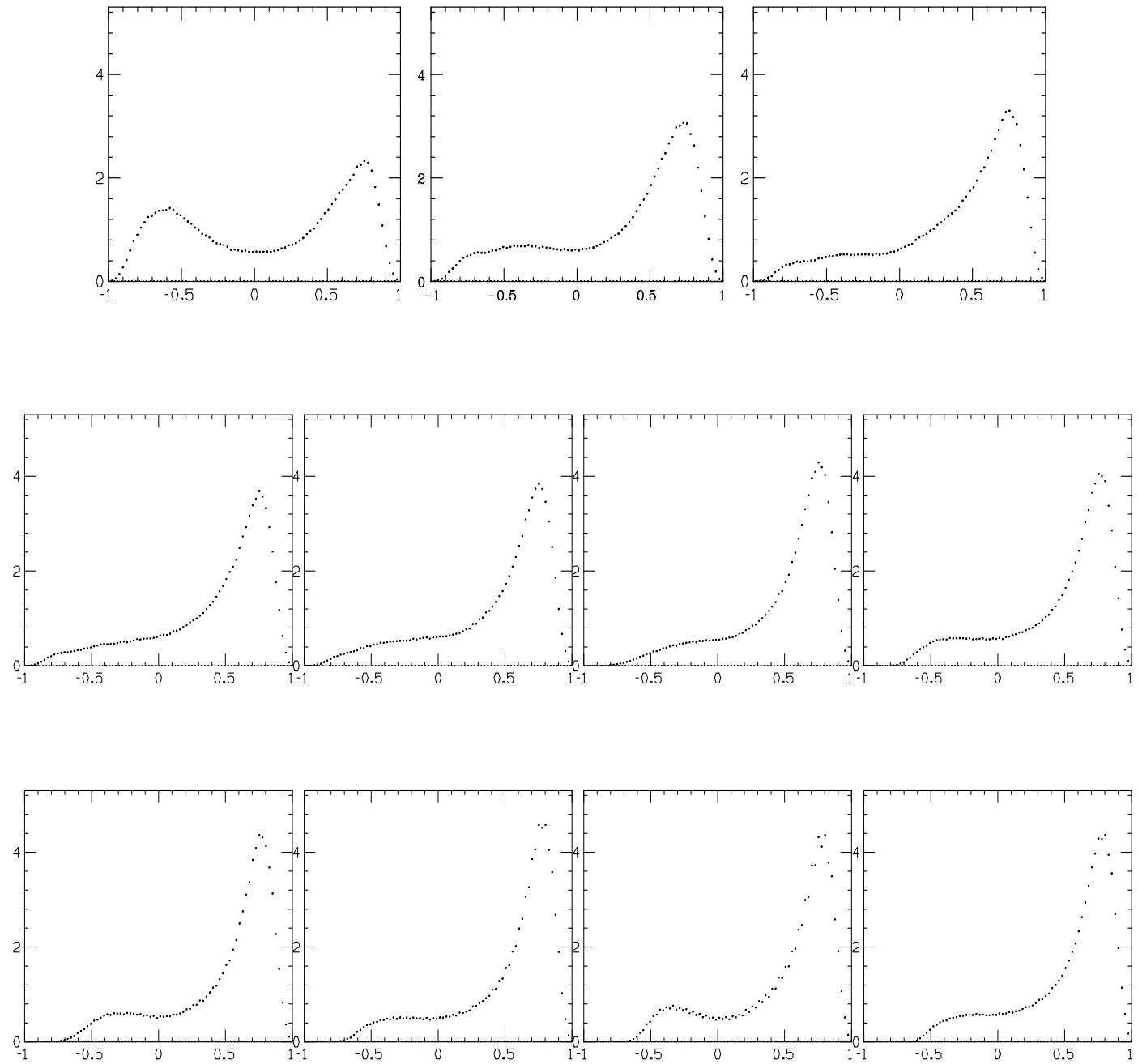
Figure 10: Evolution of the constrained P(q) (in y-axes) as a function of overlap (in x-axes) for different values of tolerance parameter ε =0.8, 0.6, 0.4, 0.3, 0.2, 0.15, 0.12, 0.1, 0.08, 0.06, 0.04. L=3, T=1.4, samples=64.
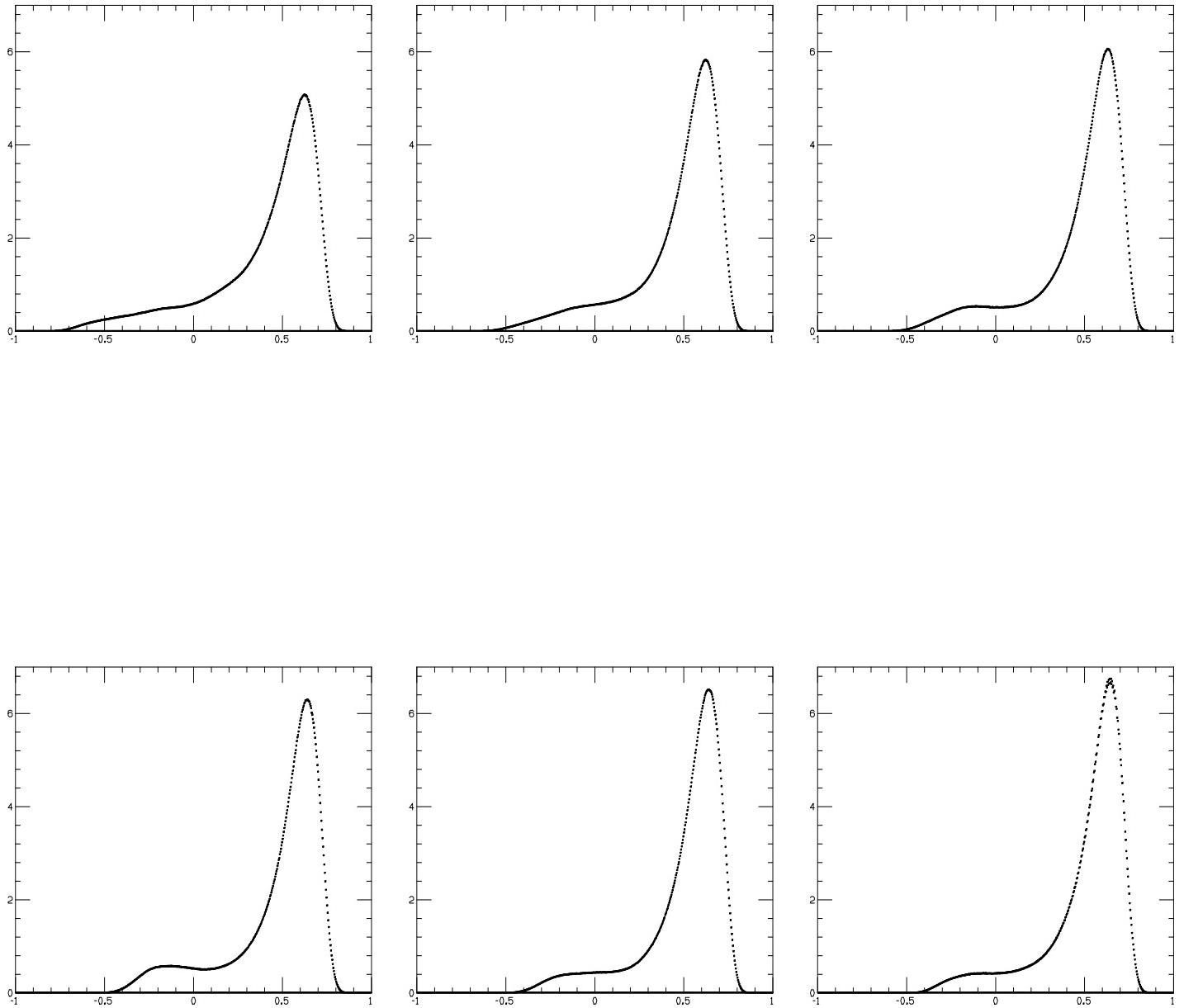
Figure 11: Evolution of constrained P(q) (in y-axes) as a function of overlap (in x-axes) for different values of tolerance parameter $\varepsilon = 0.22, 0.12, 0.09, 0.05, 0.04, 0.02$, L=5, T=1.4, samples=100.
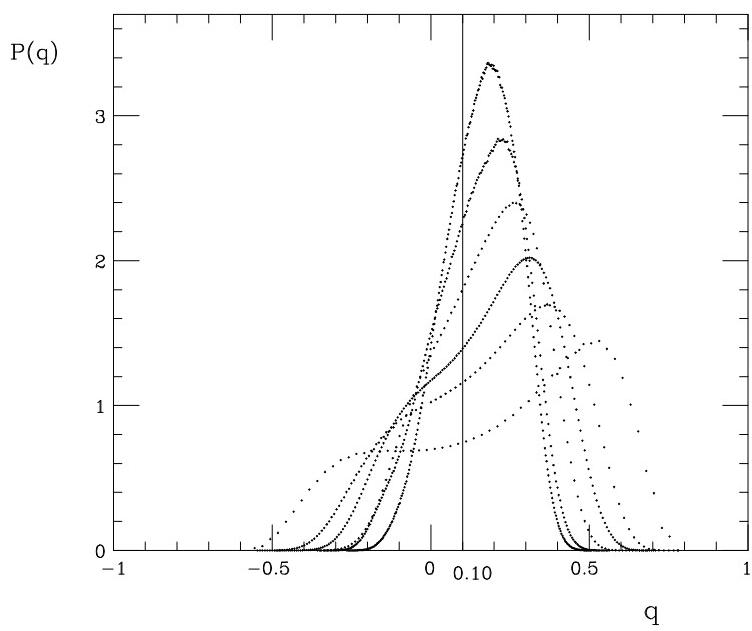
Figure 12: Study of the behaviour of constrained P(q) with lattice size; L=3, 4, 5, 6, 7, 8. T=1.4 ($q_{min} \neq q_{max}$)
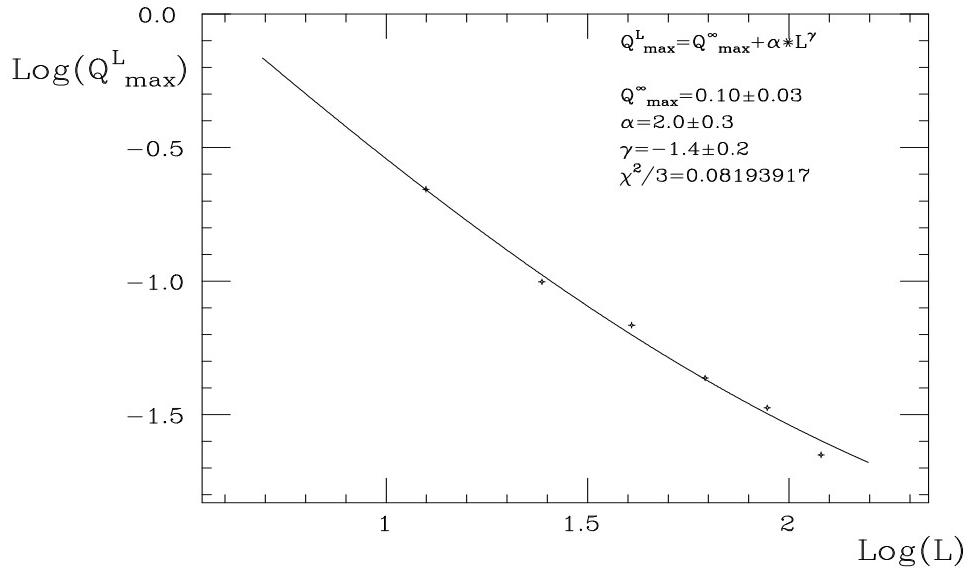
Figure 13: Fit of the predominant parameter peak of the constrained P(q) by the function $q_{max}^L = q_{max}^\infty + \frac{\alpha}{L^\gamma}$ in log-log scale
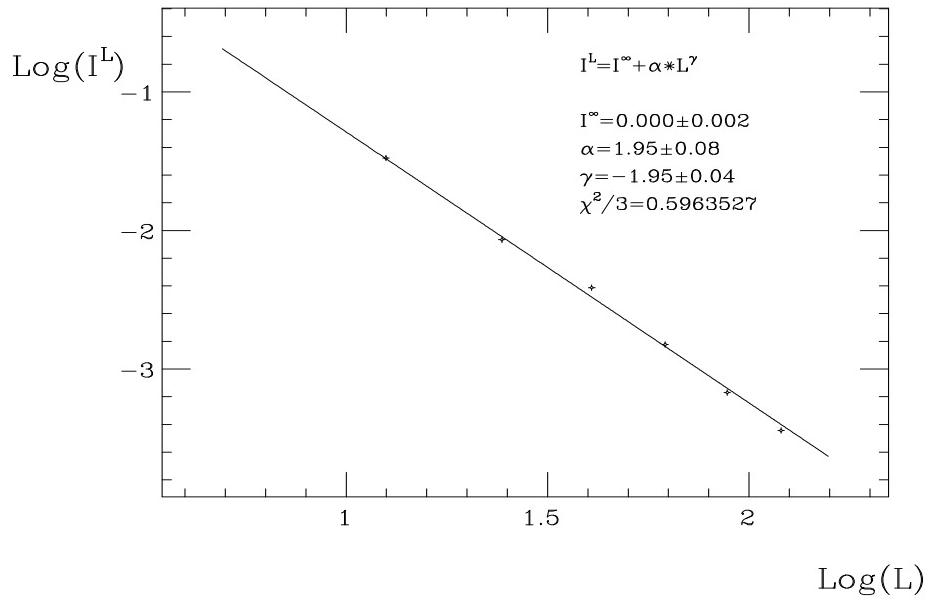

Figure 14: Evolution of the integral $I_L = \int_{-1}^{1} P_L(q_L)(q_L - 0.10)^2 dq_L$ with the lattice size in log-log scale
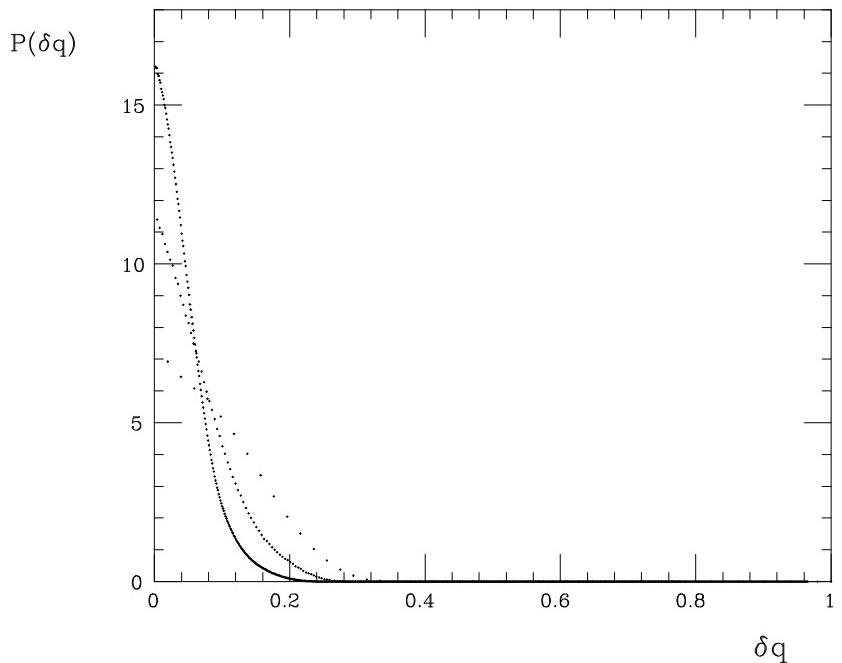
Figure 15: Ultrametric feature of the EA model for lattice of side L=4, 6 ,8. We plot the probability of the difference between the middle and the smaller overlap $\delta q = q_{mid} - q_{min}$ when the largest fall inside the range $[2/5q_{EA}, q_{EA}]$